Iranian Journal of Basic Medical Sciences

ijbms.mums.ac.ir

IJBMS

Dendrosomal nanocurcumin and p53 overexpression synergistically trigger apoptosis in glioblastoma cells

Reihaneh Keshavarz [1], Babak Bakhshinejad [1], Sadegh Babashah [1], Narges Baghi [1], Majid Sadeghizadeh [1]*

[1] Department of Molecular Genetics, Faculty of Biological Sciences, Tarbiat Modares University, Tehran, Iran

ARTICLE INFO

Article type:
Original article

Article history:
Received: Apr 29, 2016
Accepted: Jun 30, 2016

Keywords:
Apoptosis
Dendrosome
Glioblastoma
Nanocurcumin
p53
U87-MG cell line

ABSTRACT

Objective(s): Glioblastoma is the most lethal tumor of the central nervous system. Here, we aimed to evaluate the effects of exogenous delivery of p53 and a nanoformulation of curcumin called dendrosomal curcumin (DNC), alone and in combination, on glioblastoma tumor cells.

Materials and Methods: MTT assay was exploited to measure the viability of U87-MG cells against DNC treatment. Cells were separately subjected to DNC treatment and transfected with p53-containing vector and then were co-exposed to DNC and p53 overexpression. Annexin-V-FLUOS staining followed by flow cytometry and real-time PCR were applied to examine apoptosis and analyze the expression levels of the genes involved in cell cycle and oncogenesis, respectively.

Results: The results of cell viability assay through MTT indicated that DNC inhibits the proliferation of U87-MG cells in a time- and dose-dependent manner. Apoptosis evaluation revealed that p53 overexpression accompanied by DNC treatment can act in a synergistic manner to significantly enhance the number of apoptotic cells (90%) compared with their application alone (15% and 38% for p53 overexpression and DNC, respectively). Also, real-time PCR data showed that the concomitant exposure of cells to both DNC and p53 overexpression leads to an enhanced expression of GADD45 and a reduced expression of NF-κB and c-Myc.

Conclusion: The findings of the current study suggest that our combination strategy, which merges two detached gene (p53) and drug (curcumin) delivery systems into an integrated platform, may represent huge potential as a novel and efficient modality for glioblastoma treatment.

► *Please cite this article as:*
Keshavarz R, Bakhshinejad B, Babashah S, Baghi N, Sadeghizadeh M. Dendrosomal nanocurcumin and p53 overexpression synergistically trigger apoptosis in glioblastoma cells. Iran J Basic Med Sci 2016; 19:1353-1362; http://dx.doi.org/10.22038/ijbms.2016.7923

Introduction

Gliomas are brain tumors that are derived from glial tissues. Abnormal proliferation of glial cells, which normally protect neurons in the central nervous system (CNS), results in the formation of gliomas. They represent over 30% of primary brain tumors and 80% of brain malignant tumors (1). Glioblastoma multiforme (GBM), also known as glioblastoma and grade IV astrocytoma, remains by far as the most aggressive and the most prevalent tumor type in CNS pathology accounting for more than 15% of primary brain tumors in adults. The current standard therapeutic regimen for GBM patients is maximal surgical tumor resection along with postoperative adjuvant radiation therapy and chemotherapy with temozolomide (2). Complete surgical removal of the tumor could not prevent recurrence because the disease has a highly infiltrative nature. Therefore, it is very difficult for neurosurgeons to precisely pinpoint the neoplastic site and distinguish it from the surrounding healthy tissues. Despite breakthroughs in GBM detection and management, the malignancy often remains refractory to therapeutic approaches and most of the patients still have a very poor prognosis with a short mean survival (approximately 14.6 months) (3). This emphasizes the need to find more efficient strategies for glioblastoma treatment.

One of the major components of GBM malignancy is the functional status of tumor suppressor genes. p53 is one of the most important tumor suppressor genes that plays key roles in numerous cellular processes (4). This transcription factor performs its functions by transcriptionally regulating a variety of downstream target genes involved in cell cycle control, DNA repair, and programmed cell death or apoptosis (5). Although p53 is inactivated in more than half of all human cancers, and its mutation has been demonstrated to be associated with an increased risk of cancer progression, it does not become inactive in some cancers. The frequency of p53 mutation varies among different cancers ranging from 10% in hematopoietic malignancies (6) to 50-70% in head and neck (7), colorectal (8), and ovarian

*Corresponding author: Majid Sadeghizadeh. Department of Molecular Genetics, Faculty of Biological Sciences, Tarbiat Modares University,Tehran, Iran. Tel: +98-21-82884409; Fax: +98-21-82884484; email: sadeghma@modares.ac.ir

(9) tumors. Interestingly, several studies have suggested that tumors harboring wild-type 53 are defective to either induce or respond to p53 (10). As p53 contributes to the radio- and chemotherapy-mediated killing of cancer cells, enhancing its functional activity is of particular importance in tumor therapy. In this regard, p53 overexpression via exogenous p53 delivery might be suggested as a therapeutic modality with potential anti-neoplastic effects.

Curcumin is a natural hydrophobic polyphenolic compound extracted from the rhizome of the plant *Curcuma longa* (turmeric). This major active constituent of turmeric has a long history of use as a flavoring agent and herbal medicine in most Asian countries, especially India (11). Now, modern medicine has provided strong support for the idea that curcumin possesses a diverse range of therapeutic characteristics including anti-oxidant, anti-inflammatory, and anti-tumor properties (12). A growing body of evidence suggests that curcumin represents huge potential for the prevention and therapy of numerous cancer types without any discernible toxicity to normal cells (13). This substance has been revealed to trigger cell death in various cancer cell lines and to inhibit tumor growth in animal models of different malignancies (14). The potent anti-tumor activity of curcumin is reflected by its ability to suppress different steps of carcinogenesis including initiation, promotion, progression, invasion, angiogenesis, and metastasis. Curcumin fulfills its anti-cancer activities via interacting with a variety of molecular targets and signal transduction pathways involved in cancer development such as mutagenesis, cell cycle control, tumorigenesis, oncogene expression, apoptosis, and metastasis (15). Despite its well-recognized favorable pharmaceutical attributes, curcumin has some major drawbacks limiting its application as a therapeutic agent for clinical purposes. These disadvantages include low water solubility, minor cellular uptake, restricted tissue distribution, and rapid clearance from the blood leading to the overall poor bioavailability of curcumin in the body (16). Over the recent years, several strategies have been applied to surmount these obstacles and to enhance the aqueous solubility of curcumin such as the use of synthetic analogs, metabolic inhibitors, and liposomal formulations of curcumin (17). The use of nanotechnology through loading curcumin onto nanoparticles is a promising scenario in the establishment of curcumin-based anti-cancer therapeutics (18, 19). However, there has not been found any perfect formulation yet and the development of more efficient nanoparticle formulations of curcumin with a higher pharmacological efficacy is urgently needed. Dendrosome is a neutral, amphipathic, and biodegradable nanocarrier synthesized in our laboratory (20, 21), which was used as a novel nanoformulation for curcumin delivery into cells. Our previous investigations have determined various physicochemical characteristics of dendrosomal nano curcumin (DNC). Dynamic light scattering (DLS) analysis has demonstrated that the colloidal suspension of DNC is polydispersed with a mean diameter of ≤ 200 nm. Transmission electron microscopy has exhibited that DNC nanoparticles are sphere shaped. Also, *in vitro* characterization of DNC has confirmed the efficient encapsulation of curcumin in the spherical structures of dendrosome with a high loading efficiency (87%) of curcumin onto the nanocarrier. Furthermore, monitoring size and polydispersity index (PDI) over time and quantification of drug content following disruption of purified vesicles have indicated an acceptable physical and chemical stability of the drug-nanocarrier complex (22). Earlier studies in our research group on dendrosome nanoparticles have demonstrated the huge capacity of this nanocarrier for the efficient and safe delivery of hydrophobic curcumin into different cancer cells *in vitro* including epidermoid carcinoma, fibrosarcoma (19) and glioblastoma (16) cell lines. Also, the desirable therapeutic properties of our nanoformulation of curcumin have been indicated in mouse models of fibrosarcoma (19), colon cancer (23), breast cancer (24), and experimental autoimmune encephalomyelitis (EAE) (25). In the current study, we hypothesized whether the co-delivery of exogenous p53 and DNC can function in a synergistic manner to inhibit the growth of glioblastoma cells. Therefore, we examined the effects caused by p53 overexpression along with DNC treatment on U87-MG cells. The novelty of the current study is that it uses, for the first time, p53-based gene therapy together with curcumin-based drug therapy (using our synthesized nanocarrier) as an anti-tumor therapeutic strategy. This platform combines the concepts of gene therapy and drug delivery and presents a merged gene/drug delivery system with considerable potential for eradicating glioblastoma cells.

Materials and Methods

Materials and reagents

U87-MG, a human primary glioblastoma cell line, was purchased from the National Cell Bank of Iran at Pasteur Institute (Tehran, Iran). Medium and reagents for cell culture were obtained from the following sources: Dulbecco's Modified Eagle's Medium (DMEM), penicillin, and streptomycin antibiotics from GIBCO (Rockville, MD, USA), and fetal bovine serum (FBS) from HyClone (USA). Methylthiazolyldiphenyltetrazolium bromide (MTT) was prepared from Sigma-Aldrich (USA). Lipofectamine® 2000 and TRIzol were purchased from Invitrogen (USA). RNase-free DNase I was obtained from Fermentas (Lithuania). The PrimeScript™ RT kit was purchased from TAKARA BIO INC (Japan). The Annexin-V-FLUOS staining kit was obtained from Roche Applied Science (Germany). pCMV-Neo-Bam-H1-p53 plasmid, expressing human wild-type p53, was kindly provided by Dr Michael Resnick (NIEHS, NIH). To generate p53-containing

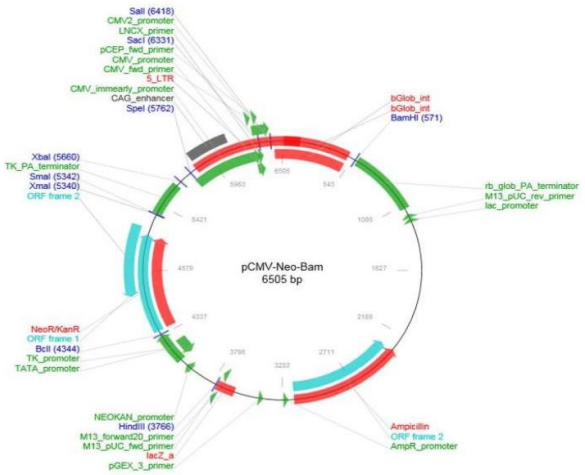

Figure 1. The map of pCMV-Neo-Bam plasmid

plasmid, the p53 cDNA was inserted into pCMV-Neo-Bam vector from Addgene (Cambridge, Massachusetts, USA). To clone the exogenous p53 gene, the plasmid was digested by the restriction enzyme BamHI. The map of pCMV-Neo-Bam plasmid is depicted in Figure 1 (accessible through https://www.addgene.org/).

DNC preparation

For DNC preparation, we used a protocol optimized in our laboratory (22). Briefly, different weight/weight ratios of dendrosome/curcumin ranging from 50:1 to 10:1 were analyzed leading to the establishment of an appropriate ratio of 25:1. Highly pure curcumin was dissolved in various amounts of dendrosome and evaluated in terms of absorbance spectrum by UV spectrophotometery (BioTek Instruments, Inc). The mixture of dendrosome and curcumin was then evaluated for excitation/emission value and compared with curcumin dissolved in phosphate-buffered saline (PBS) and 1% methanol as control. Curcumin loading onto DNC was performed using the procedure described previously (26) in which curcumin and dendrosome were co-dissolved in 5 ml of acetone followed by adding 5 ml of PBS, while stirring constantly. Acetone was evaporated by a rotary evaporator. The curcumin/dendrosome micelle solution was sterilized by using a 0.22 µm pore size syringe filter (Millex-LG, Millipore Co, USA). Finally, the prepared DNC was stored at 4 ˚C in a light-protected condition until use. For *in vitro* experiments, DNC was diluted in complete culture medium as mentioned for each assay.

Cell culture

Tumor cells were grown in DMEM supplemented with 10% FBS, penicillin (100 U/ml), streptomycin (100 mg/ml), and 2 mM L-glutamine. Cells were cultured in 25 cm^2 polystyrene culture flasks or multi-well culture plates in order to reach sub-confluent monolayers. The cells in culture were maintained at 37 ˚C in a humidified atmosphere containing 95% air and 5% CO_2. For routine maintenance, cells were trypsinized and passaged before becoming fully confluent. Cells were not kept in continuous culture for more than 1.5 months.

Cell viability assay

MTT colorimetric assay was performed to measure the toxicity of DNC to U87-MG cells and to determine cell viability. Briefly, growing cells were seeded onto 96-well plates (8×10^3 cells/well for 24 hr and 5×10^3 cells/well for 48 hr) and allowed to attach overnight. Afterwards, cells were treated with various concentration of DNC (0, 8, 15, 17, 20, 25, 30, 35, 40 and 45 µM). Treatment agent was carefully removed from wells, and cells were washed twice with PBS. After incubating for 24 and 48 hr, 20 µl of MTT reagent (5 mg/ml) was added to each well, and cells were further incubated at 37 °C for 4 hr. The supernatant was completely removed and 200 µl of dimethyl sulfoxide (DMSO) solution was added to wells. The multi-well plate was then placed for 10 min in a dark place. The optical density of DMSO-dissolved formazan salts was measured at 490 nm using a microtiter plate reader (Biotek, USA). All values were compared to the corresponding controls. Cell viability was calculated as ratio of the absorbance of treated cells to untreated control cells. The following formula was used for determining the percentage of viable cells in MTT assay (27).

$$\text{Viable cells (\%)} = \frac{\text{OD}\boldsymbol{t}}{\text{OD}\boldsymbol{u}} \times 100$$

In this equation, ODt represents the absorbance value of treated sample and ODu represents the absorbance value of corresponding untreated sample.

Cell transfection

One day before transfection, cells were seeded onto 12-well plates and cultured in growth medium without antibiotic. The appropriate confluency was 80% at the time of transfection. Lipofectamine® 2000 was used as transfection reagent. Cells were transfected with plasmid DNA (pDNA) containing p53 gene according to the manufacturer's instructions. The transfection procedure was optimized in order to reach transfection protocol with the highest efficiency. The optimal concentration of p53-containing plasmid was determined 100 ng/µl. This concentration was applied to all transfection tests. To form pDNA:lipofectamin complex, plasmid and transfection reagent were incubated for 30 min at room temperature, and the complexes were added to the corresponding wells. Insertless vector (plasmid without p53) encapsulated by lipofectamine was used as control. Also, cells exposed only to lipofectamine were used as positive control. 48 hr after transfection, cells were treated with DNC (according to

Table 1. The oligonucleotide primers used in real-time PCR; *GAPDH* was used as a housekeeping gene

Gene		Primer sequence (5′→3′)	Amplicon size
P53	F	TCCTCAGCATCTTATCCGAGTG	265
	R	AGGACAGGCACAAACACGCACC	
GADD45	F	GGAGAGCAGAAGACCGAAAGG	152
	R	AGCAGGCACAACACCACGT	
NF-κB	F	TACTCTGGCGCAGAAATTAGGTC	265
	R	ACTGTCTCGGAGCTCGTCTATTTG	
c-Myc	F	CTCCTACGTTGCGGTCACAC	142
	R	CGGGTCGCAGATGAAACTCT	
GAPDH	F	ACACCCACTCCTCCACCTTTG	112
	R	TCCACCACCCTGTTGCTGTAG	

F =Forward primer; R =Reverse primer; GAPDH, Glyceraldehyde 3-phosphate dehydrogenase

the IC_{50} concentration obtained from MTT assay).

RNA isolation and reverse transcription PCR

Total RNA was isolated from cultured cells using TRIzol reagent according to the manufacturer's instructions. Total RNA was treated with RNase-free DNase I digestion. Single-stranded complementary DNA (cDNA) was synthesized using PrimeScript™ RT kit. The cDNA was then amplified through PCR, which was performed for 30 cycles under the following conditions: 95 ˚C for 20 sec, 58 ˚C for 20 sec, 72 ˚C for 30 sec, preceded by an initial denaturation at 95 ˚C for 5 min and followed by a final extension at 72 ˚C for 5 min. Finally, the PCR products were electrophoresed on 1.5% agarose gel.

Apoptosis assay

The Annexin-V-FLUOS staining kit was used to measure the number of apoptotic cells. Apoptosis is detected based on changes that occur in the cell membrane. Annexin V binds to phosphatidylserine molecules exposed on the outer leaflet of the plasma membrane lipid bilayer of the cells entered the apoptotic pathway. In brief, cells were seeded onto six-well plates (0.3×10^6 cells/well) and incubated at 37 ˚C for 24 hr. U87-MG cells were harvested by trypsinization. The trypsin-digested cells were pelleted by centrifugation (1500 rpm for 6 min), and washed by ice-cold PBS. The cell pellet was resuspended in 100 µl of 1X Annexin-binding buffer and 100 µg/ml of propidium iodide (PI) working solution and then incubated in the dark for 10–15 min. Afterwards, the stained cells were immediately analyzed by flow cytometry (BD FACSCanto II flowCytometer, USA). Early apoptotic cells were determined by positive staining for Annexin V-FITC and late apoptotic cells were determined by positive staining for both Annexin V-FITC and PI.

Quantitative real-time PCR

Quantitative PCR was performed using SYBR® Premix Ex Taq (Takara, Japan) on Step One ABI Sequence Detection System (Applied Biosystems, Foster City, CA) in 96-well microtiter plates. Real-time PCR reaction was carried out in final volumes of 15 µl with 1 ng of cDNA template, 7.5 µl of SYBER Green master mix, and 0.4 nM of forward and reverse primers. Amplification was performed as follows: initial denaturation at 95 ˚C for 5 min followed by 40 cycles of denaturation at 95 ˚C for 30 sec, annealing at 60 ˚C for 30 sec, and extension at 72 ˚C for 30 sec. The specificity of PCR products was examined by electrophoresis on 1.5% agarose gel to verify their size and dissociation curve analysis. Melt curve analysis was performed after each run to confirm the lack of primer dimers. Different concentrations of cDNA were prepared to determine the efficiency of each primer set. RT-PCR results were normalized by the housekeeping gene glyceraldehyde-3-phosphate dehydrogenase (GAPDH). The relative expression for each gene was calculated by $2^{-\Delta\Delta CT}$ method, where ΔCt=mCt (gene of interest) -mCt (housekeeping gene) and ΔΔCt=ΔCt (control group) -ΔCt (treated group). The sequences of forward and reverse primers used in real-time PCR reactions are listed in Table 1. The primers were designed by Gene Runner software.

Statistical analysis

Data were analyzed by GraphPad Prism 5 software (GraphPad Software, Inc, La Jolla, CA, USA). Unpaired t-test was used for statistical analyses and $P<0.05$ was considered as significant.

Results

DNC dramatically decreases the viability of U87-MG cells

The sensitivity of U87-MG cells to DNC was measured by MTT assay. To investigate DNC toxicity, cells were incubated with different concentrations of DNC at different time intervals (24 and 48 hr). As shown in Figure 2, DNC significantly inhibits the proliferation of U87-MG cells in a time- and dose-dependent manner. The half maximal inhibitory concentration (IC_{50}) of DNC for U87-MG cells was 27.5 µM after 24 hr (Figure 2A), which was reduced to 15 µM after 48 hr (Figure 2B). Also, microscopic visualization exhibited dramatic morphological changes in the cells treated with DNC (Figure 2C). This altered cell morphology may implicitly indicate the occurrenc

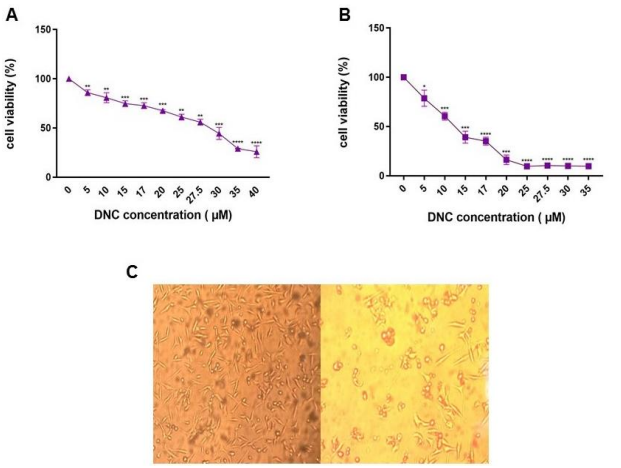

Figure 2. DNC effects on the viability of U87-MG cells. (A-B) Cells were exposed to different concentrations of DNC for 24 (A) and 48 hr (B). DNC results in a reduced population of cancer cells in a time- and concentration-dependent mode. The results are expressed as the mean ± standard deviation: **P*<0.05; ** *P*<0.01; *** *P*<0.001 (in comparison with control cells which were not treated with DNC). (C) A microscopic view from U87-MG cells before (left) and after (right) being treated with DNC (100X magnification)

of cell death (irrespective of its type). Overall, our results demonstrated that increasing the concentration of DNC as well as enhancing the incubation time of cells with DNC leads to the reduction of the viability of cancer cells that is detected by a reduced number of viable cells. Also, the IC_{50} values of DNC for glioblastoma cells obtained from MTT assay were used for further experiments.

p53 overexpression and DNC act synergistically to induce apoptosis in U87-MG cells

To determine the mode of cell death, Annexin-V-FLUOS and PI staining were used. Staining the cells with Annexin V and PI could distinguish apoptosis from necrosis, which is known as another common mode of cell death. The percentage of apoptotic cells was calculated by Annexin V-FITC and PI staining followed by flow cytometry. As indicated in Figure 3, the number of apoptotic cells was 2% in control sample with no treatment. It was observed that there is a marked increase in the ratio of U87-MG cells undergoing apoptosis when the cells are exposed to treatment with DNC or p53 overexpression. DNC treatment and p53 overexpression enhanced the percentage of late apoptotic cells to 38% and 15%, respectively. Interestingly, when U87-MG cells were concomitantly treated with DNC and transfected with p53-containing vector, the population of apoptotic cells showed a significant elevation and reached 90%. The results of apoptosis assay obviously demonstrated that p53 overexpression and DNC treatment can act in a synergistic manner to

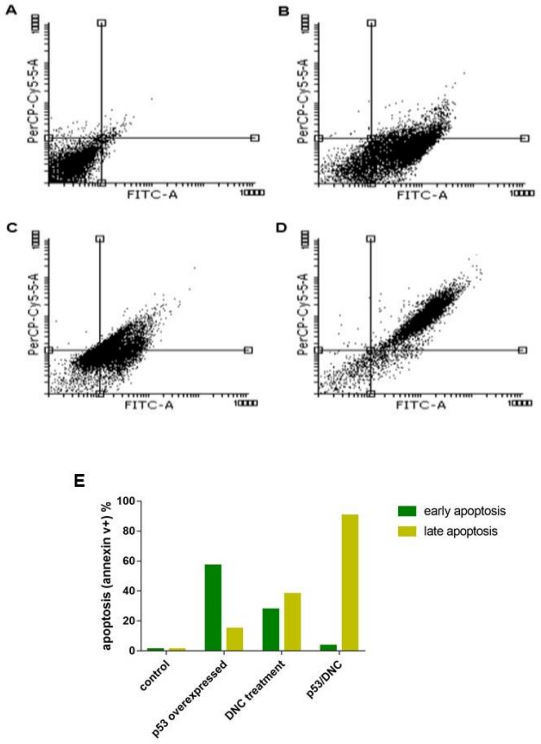

Figure 3. Synergistic functions of p53 overexpression and DNC treatment in inducing apoptosis in U87-MG cells. (A-D) The results of flowcytometry: Viable cells (Annexin-V-/PI-), early apoptotic cells (Annexin-V+/PI-), late apoptotic cells (Annexin-V-/PI+), and necrotic cells (Annexin-V+/PI+) are located in the lower left, lower right, upper right, and upper left quadrants, respectively. (E) Graphic representation of the percentage of apoptotic cells for control, p53 overexpressed, DNC treated and p53 overexpressed + DNC treated samples. When cells are both treated with DNC and transfected with p53, the number of cells undergoing apoptosis is significantly increased compared with the condition when cells are exposed to DNC treatment or p53 overexpression alone. PI: Propidium iodide

enhance apoptosis in U87-MG tumor cells and thus their concomitant application can lead to apoptosis significantly higher than their use alone.

Concomitant application of DNC treatment and p53 overexpression alters the expression levels of NF-κB, c-Myc and GADD45

Alterations in the expression levels of p53, GADD45, NF-κB, and c-Myc were analyzed by real-time PCR. The gene expression levels were examined in 4 groups including control (cells with no treatment), DNC+ (cells treated with DNC), p53 overexpressed (cells with p53 overexpression), and DNC+/p53 overexpressed (cells with both DNC treatment and p53 overexpression). The housekeeping gene GAPDH was used as internal control to normalize the expression levels of different genes. As depicted in Figure 4, our results exhibited that DNC treatment causes a significant increase in the mRNA levels of p53 and GADD45 (*P*<0.01), but a marked decrease was observed in the mRNA levels of NF-κB and c-Myc (*P*<0.001) compared with control. On the other hand, transfection of cells with p53-containig

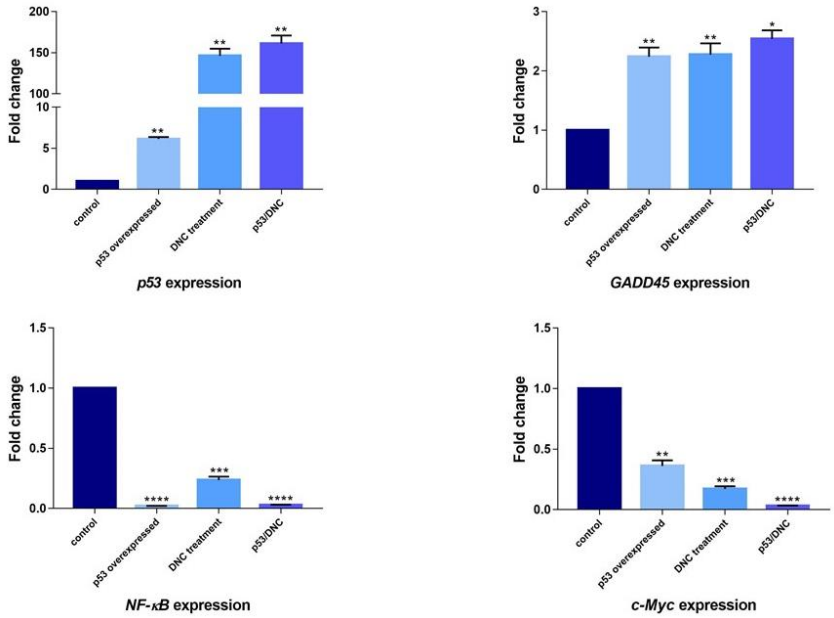

Figure 4. Effects of DNC treatment and p53 overexpression on the mRNA levels of cell cycle genes (p53 and GADD45) and oncogenes (NF-κB and c-Myc). When U87-MG cells are simultaneously exposed to treatment with DNC and transfected with p53-expressing vector, they show a higher upregulation of p53 and a stronger down-regulation of NF-κB and c-Myc than single use of DNC or p53 overexpression. Data are indicated as fold change in relative expression compared with GAPDH on the basis of comparative $2^{-\Delta\Delta Ct}$ method and expressed as the mean ± standard deviation; * P<0.05; ** P<0.01; *** P<0.001

vector significantly enhanced the mRNA levels of p53 and GADD45 (P < 0.01) and reduced the mRNA levels of NF-κB and c-Myc (P < 0.001 and P < 0.01, respectively) in comparison with control. However, when U87-MG cells were both treated with DNC and transfected with p53-expressing vector, they indicated a significant enhancement in the expression levels of p53 and a significant reduction in the expression levels of NF-κB and c-Myc compared with cell exposure to either DNC treatment or p53 overexpression alone. GADD45 showed a varying expression profile in DNC +/p53 overexpressed versus DNC+ and p53 overexpressed cells. Taken together, the results of quantitative real-time PCR indicated that concomitant exposure of cells to both DNC and p53 overexpression leads to an enhanced expression of the cell cycle gene p53 and a reduced expression of NF-κB and c-Myc in comparison with condition in which cells are subjected to DNC or p53 overexpression alone. These findings suggest that combined application of DNC treatment and p53 overexpression can be used as an anti-tumor strategy for the treatment of glioblastoma cancer cells and is more efficient in fighting glioblastoma compared with using curcumin therapy or re-activating p53 alone.

Discussion

Glioblastoma multiforme (GBM) accounts for the most lethal primary brain tumors with a very poor prognosis. Despite advances in different treatments such as chemotherapy, surgery and radiotherapy, the survival rate of patients with glioblastoma is low. Therefore, there has been much interest in the development of new therapeutic strategies for GBM to improve the survival of patients. Nanotechnology has emerged as a potential platform for cancer treatment that is able to bolster the effects caused by different therapeutic interventions including gene therapy, chemotherapy, etc. Nanotechnology provides the opportunity for the production of gene and drug delivery systems with a small particle size, which are called nanocarriers. Dendrosome is a novel bio-degradable and amphipathic nanocarrier synthesized by our research group (21). This nanocarrier has been demonstrated to present enormous efficacy as a gene porter and drug delivery platform in various studies *in vitro* and *in vivo* (19, 23, 25, 28). In the current work, we used OA400 dendrosome as a nanocarrier for curcumin delivery into U87-MG glioblastoma cells. The efficiency of this nanocarrier for tumor drug delivery has been indicated in previous reports of our laboratory (16, 29). To reach an optimized therapeutic modality for brain tumor cells, we combined dendrosome-based curcumin delivery (in the form of DNC) with a gene therapy approach based on the delivery of exogenous p53 into target cancer cells.

In our earlier report, it has been shown that the effective doses of dendrosomal nanocarrier for anti-cancer drug delivery do not exert any toxic effects on normal human cells (16). In this context, in concentrations that are suppressive for cancer cell growth, no harmful effect associated with DNC has been found in stem cells and normal fibroblast cells. In our work, MTT assay was applied to quantitatively determine the viability of U87-MG cells against DNC

treatment. The incubation of glioblastoma cells with different DNC concentrations revealed that DNC inhibits the growth and proliferation of U87-MG cells in a time- and concentration-dependent manner. Both the decreased number of viable cells - determined by MTT - and the severely impaired morphology of cells treated with the drug - determined by microscopic visualization - suggest that DNC treatment can lead to the death of U87-MG cells. The IC_{50} of DNC, obtained from MTT assay, was selected as an appropriate concentration for further experiments. Consistent with MTT data, staining the cells with Annexin-V and PI indicated that both DNC treatment and p53 overexpression can singly drive U87-MG cells toward apoptosis. However, our combination approach, which is based on the simultaneous exploitation of dendrosome-mediated curcumin delivery and p53 transfection, proves to be much more efficient in inducing apoptosis. This observation leads us to the conclusion that although each of the above-mentioned approaches has been suggested as a strategy for treating glioblastoma, our combination approach seems to present a higher therapeutic index. This better outcome might be attributed to the synergism of the two methods. This synergistic function triggers a more efficacious activation or inhibition of the intracellular pathways they can modulate separately in glioblastoma cells. The observation of higher degrees of apoptosis in combined application of DNC treatment and p53 overexpression can be explained by the biological function of p53 when cells are subjected to stress signals. Under normal unstressed conditions, the p53 level is very low because of Mdm2 binding and ensuing degradation. In response to cellular stress signals such as DNA damage (induced by anti-cancer drugs such as curcumin), p53 becomes dissociated from Mdm2 and is activated. Once activated, p53 blocks cell cycle progression. p53-dependent cell cycle arrest provides enough time for DNA damage to be repaired. If DNA damage is extreme and beyond repair, p53 triggers apoptosis in order to inhibit the transfer of new mutations to daughter cells (30).

The findings of the current work indicate that p53-associated signaling plays an important role in apoptosis induced by curcumin. Our results agree well with previous reports in which p53 activation (31-33) as well as curcumin (34-36) has been shown to have independently the capacity for apoptosis induction. The role of curcumin in triggering apoptosis has been investigated in numerous studies, and there is a range of evidence demonstrating its potential to activate different pathways related to apoptosis. Interestingly, it has been revealed that curcumin-mediated apoptosis induction in cancer cells occurs in a p53-dependent mode. For example, treatment of human basal cell carcinoma cells (BCC) with curcumin leads to apoptosis accompanied by the upregulation of p53 protein and its downstream targets including GADD45. Also, transfection of cells with a p53-specific antisense oligonucleotide causes an attenuated curcumin-induced apoptosis (37).

In the current work, we observed significantly far decreased levels of NF-κB and c-Myc after exposure of U87-MG cells to the combination approach compared with individual use of DNC treatment or p53 overexpression. These data are supported by reports on the established role of p53-mediated effect of curcumin on the negative regulation of NF-κB and its downstream targets. Previous studies have suggested that the inhibition of NF-κB activation by curcumin can result in the inhibition of proliferation of various malignancies including prostate cancer, mantel cell lymphoma, multiple myeloma, ovarian cancer, melanoma, pancreatic cancer, head and neck squamous cell carcinoma (HNSCC), bladder cancer, glioblastoma and lung cancer (38-40). In fact, NF-κB is a crucial component of the regulatory network through which curcumin exerts its effects on target cells. Both anti-tumor and anti-inflammatory properties of curcumin have been found to be mediated via downregulating the transcription factor NF-κB and NF-κB-regulated gene products. The down-regulation of NF-κB and its downstream targets contributes to the sensitization of tumor cells to radio- and chemotherapy. c-Myc is also another downstream target, which is positively controlled by NF-κB. Therefore, we observed that the reduced levels of NF-κB are accompanied by c-Myc down-regulation.

The rationale behind using GADD45, NF-κB and c-Myc in the current study can be explained by the significant roles played by these molecules in apoptosis regulation. A vast majority of studies have suggested that NF-κB acts in the upstream cellular pathways of apoptosis. Also, there is a large body of evidence supporting the notion that GADD45 variants are master switches in determining the cell fate with regard to life and death decisions in cancer cells (41). This defining role of GADD45 as a mediator of survival or apoptosis is closely linked to NF-κB and c-Myc. The anti-apoptotic activity of NF-κB/IκB signaling pathway in promoting cell survival has been observed in response to various apoptotic stimuli. The role of NF-κB as an important anti-apoptotic molecule is backed by convincing results obtained from *in vitro* and *in vivo* studies. Neurodegenerative diseases, characterized by excessive pathologic apoptosis, are considered as appropriate models for *in vitro* studies. In this context, NF-κB has been indicated to protect cortical neurons from apoptosis induced by β-amyloid peptides (42, 43). These peptides are known as the causal agents in the pathogenesis of Alzheimer's diseases. Also, *in vivo* studies are of utmost importance in this regard. These studies are based

on animal models in which genes encoding the NF-κB family members or upstream kinases are disrupted. These gene knockout models have indicated the death of mice before birth and during different stages of embryonic development (44). Also, the investigation of rodent models of stroke has demonstrated that NF-κB could prevent ischemic neuronal degeneration. This protective role is attributed to the NF-κB-mediated transcription of anti-apoptotic factors such as Bcl-2 (45). On the functional level, there is a mutual direct cross-competition between p53, a major pro-apoptotic protein, and NF-κB. Furthermore, a variety of anti-apoptotic genes are targeted by NF-κB that include the cell-cycle regulatory protein cyclin D1, the mitochondrial membrane-stabilizing proteins Blf-1, Bcl-xl (a Bcl-2 family member), the caspase inhibitors cIAP1, cIAP2 and XIAP, and TNF receptor-associated factors TRAF1 and TRAF2 (46). The NF-κB-mediated upregulation of these proteins might be considered as a means for the cell to escape apoptosis.

GADD45 functions as an upstream effector in the cellular apoptotic program. GADD45 is transcriptionally regulated by p53. This occurs through different routes including p53 binding to a conserved site within the third intron of one of the GADD45 variants (47) and binding of the p53-interacting transcription factors WT1 and Egr-1 to the GADD45 promoter (48). But, in addition to being regulated by p53, GADD45 also activates p53 via p38. Interestingly, DNA damage seems to play a determining role in mutual regulation of p53 and GADD45. It is believed that p38-p53-GADD45 forms a stress-activated regulatory loop in cancer cells (48). GADD45 can also activate p53 via JNK-mediated phosphorylation. This activation takes place after DNA damage and has been shown to be essential for the stabilization of a mutant form of p53, thereby mediating an apoptosis response (49). In this context, p53 and GADD45 act in a co-dependent manner. This co-dependence is further favored by the fact that GADD45 null mice suppress p53 phosphorylation, and cultured cells treated with p53 inhibitors exhibit reduced levels of GADD45 induction. Also, GADD45 null skin and keratinocyte cell lines indicate compromised activation of p38, JNK, and p53 as well as resistance to p53-induced apoptosis (50). The activation of both p38 and JNK by GADD45 leading to apoptosis is mediated by direct interaction of GADD45 with MEKK4. (MAPK extracelluar signal-regulated kinase kinase 4) Furthermore, GADD45 is able to interact with Bcl-2, which is followed by activation of the pro-apoptotic factor Bax. Activated Bax increases the cytochrome-c release into the cytoplasm and finally triggers apoptosis (51). Therefore, different studies confirm the association of GADD45 with apoptosis, especially after oncogenic and genotoxic stress (such as DNA damage). These reports suggest the activation of GADD45 in cancer cells as an efficient means for inducing apoptosis. Down-regulation of GADD45 is recognized as an essential step for various cancer types to escape apoptosis. In addition, the inhibition of NF-κB has been demonstrated to upregulate GADD45 leading to apoptosis induction and prevention of tumor growth. Of note, c-Myc is an important player in the NF-κB-induced regulation of GADD45. It has been revealed that NF-κB upregulates c-Myc, which in turn results in GADD45 down-regulation. This occurs via c-Myc interaction with regulatory sequences in the promoter of GADD45.

Due to the significance of p53 and its connections with NF-κB, c-Myc, and GADD45 in regulating apoptosis, these apoptosis-associated molecules can serve as prime targets for therapeutic intervention of cancer. Analyzing changes in the expression levels of these factors in response to external stimuli is of particular importance for the development of apoptosis-oriented anti-cancer strategies. The current study could result in a better and more detailed understanding of the molecular mechanisms involved in the pro-apoptotic activity of p53 overexpression and DNC in brain tumor cells with regard to NF-κB, c-Myc, and GADD45. This information can offer rich and fundamental insight into the combined use of curcumin therapy - as a highly effective chemoprevenitve modality- and p53 gene therapy.

Conclusion

The novelty of the current study is to combine a gene therapy approach (p53 transfection) with a drug delivery strategy for killing U87-MG cells. This combination gene/drug delivery platform can improve the therapeutic efficiency and anti-tumor efficacy for fighting highly aggressive glioblastoma cells. The safety of our anti-tumor drug-nanocarrier formulation (DNC) toward normal cells is of particular importance for *in vivo* studies as well as for ultimate translation of these findings to the clinical setting. Thus far, merged gene/drug delivery systems have been largely ignored in the field of anti-cancer studies. However, the unification of detached gene and drug delivery systems into an integrated package can present new perspectives to the landscape of cancer research. The next goal will be to develop a joint delivery platform in which gene delivery and drug delivery components are physically tethered together. This can be achieved by encapsulation of the p53-expressing plasmid in dendrosomal nanocarriers. In this context, dendrosome is able to carry both the therapeutic gene (p53 or any other gene with therapeutic

potential) and the desired chemotherapeutic drug. Studies such as our work seem promising to fulfill this purpose and can pave the way for reframing a new doctrine of brain cancer therapy.

Acknowledgment

We gratefully acknowledge our colleagues in Department of Genetics (Tarbiat Modares University, Tehran, Iran) for their helps in doing the current research. This work was supported financially by a research grant from Tarbiat Modares University. The results described in this paper were part of student thesis.

Conflict of interest

The authors declare that there is no conflict of interest.

References

1. Meng J, Li P, Zhang Q, Yang Z, Fu S. A radiosensitivity gene signature in predicting glioma prognostic via EMT pathway. Oncotarget 2014; 5:4683-4693.
2. Chinot OL, Wick W, Mason W, Henriksson R, Saran F, Nishikawa R, *et al*. Bevacizumab plus radiotherapy-temozolomide for newly diagnosed glioblastoma. N Engl J Med 2014;370:709-722.
3. Sa JK, Yoon Y, Kim M, Kim Y, Cho HJ, Lee JK, *et al*. In vivo RNAi screen identifies NLK as a negative regulator of mesenchymal activity in glioblastoma. Oncotarget 2015; 6:20145-59.
4. Tang Y, Zhao W, Chen Y, Zhao Y, Gu W. Acetylation is indispensable for p53 activation. Cell 2008; 133:612-626.
5. Badie B, Goh CS, Klaver J, Herweijer H, Boothman DA. Combined radiation and p53 gene therapy of malignant glioma cells. Cancer Gene Ther 1999; 6:155-162.
6. Peller S, Rotter V. TP53 in hematological cancer: low incidence of mutations with significant clinical relevance. Hum Mutat 2003; 21:277-284.
7. Blons H, Laurent-Puig P. TP53 and head and neck neoplasms. Hum Mutat 2003;21:252-257.
8. Iacopetta B. TP53 mutation in colorectal cancer. Hum Mutat 2003; 21:271-276.
9. Schuijer M, Berns EM. TP53 and ovarian cancer. Hum Mutat 2003; 21:285-291.
10. Sun Y. E3 ubiquitin ligases as cancer targets and biomarkers. Neoplasia 2006; 8:645-654.
11. Lee SJ, Krauthauser C, Maduskuie V, Fawcett PT, Olson JM, Rajasekaran SA. Curcumin-induced HDAC inhibition and attenuation of medulloblastoma growth *in vitro* and *in vivo.* BMC Cancer 2011; 11:144.
12. Choi BH, Kim CG, Bae YS, Lim Y, Lee YH, Shin SY. p21 Waf1/Cip1 expression by curcumin in U-87MG human glioma cells: role of early growth response-1 expression. Cancer Res 2008; 68:1369-1377.
13. Alizadeh AM, Sadeghizadeh M, Najafi F, Ardestani SK, Erfani-Moghadam V, Khaniki M, *et al*. Encapsulation of curcumin in diblock copolymer micelles for cancer therapy. Biomed Res Int 2015; 2015:824746.
14. Kunnumakkara AB, Anand P, Aggarwal BB. Curcumin inhibits proliferation, invasion, angiogenesis and metastasis of different cancers through interaction with multiple cell signaling proteins. Cancer Lett 2008; 269:199-225.
15. Dudas J, Fullar A, Romani A, Pritz C, Kovalszky I, Hans Schartinger V, *et al*. Curcumin targets fibroblast-tumor cell interactions in oral squamous cell carcinoma. Exp Cell Res 2013; 319:800-809.
16. Tahmasebi Mirgani M, Isacchi B, Sadeghizadeh M, Marra F, Bilia AR, Mowla SJ, *et al*. Dendrosomal curcumin nanoformulation downregulates pluripotency genes via miR-145 activation in U87MG glioblastoma cells. Int J Nanomed 2014; 9:403-417.
17. Orr WS, Denbo JW, Saab KR, Myers AL, Ng CY, Zhou J, *et al*. Liposome-encapsulated curcumin suppresses neuroblastoma growth through nuclear factor-kappa B inhibition. Surgery 2012; 151:736-744.
18. Bisht S, Feldmann G, Soni S, Ravi R, Karikar C, Maitra A, *et al*. Polymeric nanoparticle-encapsulated curcumin ("nanocurcumin"): a novel strategy for human cancer therapy. J Nanobiotechnol 2007; 5:3.
19. Babaei E, Sadeghizadeh M, Hassan ZM, Feizi MA, Najafi F, Hashemi SM. Dendrosomal curcumin significantly suppresses cancer cell proliferation *in vitro* and *in vivo.* Int Immunopharmacol 2012; 12:226-234.
20. Sadeghizadeh M, Ranjbar B, Damaghi M, Khaki L, Sarbolouki MN, Najafi F, *et al*. Dendrosomes as novel gene porters-III. J Chem Technol Biotechnol 2008; 83:912-920.
21. Sarbolouki MN, Sadeghizadeh M, Yaghoobi MM, Karami A, Lohrasbi T. Dendrosomes: a novel family of vehicles for transfection and therapy. J Chem Technol Biotechnol 2000; 75:919-922.
22. Mirgani MT, Isacchi B, Sadeghizadeh M, Marra F, Bilia AR, Mowla SJ, *et al*. Dendrosomal curcumin nanoformulation downregulates pluripotency genes via miR-145 activation in U87MG glioblastoma cells. Int J Nanomed 2014; 9:403-417.
23. Alizadeh AM, Khaniki M, Azizian S, Mohaghgheghi MA, Sadeghizadeh M, Najafi F. Chemoprevention of azoxymethane-initiated colon cancer in rat by using a novel polymeric nanocarrier--curcumin. Eur J Pharmacol 2012; 689:226-232.
24. Farhangi B, Alizadeh AM, Khodayari H, Khodayari S, Dehghan MJ, Khori V, *et al*. Protective effects of dendrosomal curcumin on an animal metastatic breast tumor. Eur J Pharmacol 2015; 758:188-196.
25. Mohajeri M, Sadeghizadeh M, Najafi F, Javan M. Polymerized nano-curcumin attenuates neurological symptoms in EAE model of multiple sclerosis through down regulation of inflammatory and oxidative processes and enhancing neuroprotection and myelin repair. Neuropharmacology 2015; 99:156-167.
26. Gou M, Men K, Shi H, Xiang M, Zhang J, Song J, *et al*. Curcumin-loaded biodegradable polymeric micelles for colon cancer therapy *in vitro* and *in vivo.* Nanoscale 2011; 3:1558-1567.
27. Lai Lh, Fu Qh, Liu Y, Jiang K, Guo Qm, Chen Qy, *et al*. Piperine suppresses tumor growth and metastasis

in vitro and *in vivo* in a 4T1 murine breast cancer model. Acta Pharmacol Sin 2012; 33:523-5230.
28. Massumi M, Ziaee AA, Sarbolouki MN. Apoptosis induction in human lymphoma and leukemia cell lines by transfection via dendrosomes carrying wild-type p53 cDNA. Biotechnol Lett 2006;28(1):61-6.
29. Dehghan Esmatabadi MJ, Farhangi B, Safari Z, Kazerooni H, Shirzad H, Zolghadr F, *et al*. Dendrosomal curcumin inhibits metastatic potential of human SW480 colon cancer cells through Down-regulation of Claudin1, Zeb1 and Hef1-1 gene expression. Asian Pac J Cancer Prev 2015; 16:2473-2481.
30. Sun Y. p53 and its downstream proteins as molecular targets of cancer. Mol Carcinog 2006; 45:409-415.
31. Fridman JS, Lowe SW. Control of apoptosis by p53. Oncogene 2003; 22:9030-9040.
32. Amaral JD, Xavier JM, Steer CJ, Rodrigues CM. The role of p53 in apoptosis. Discov Med 2010; 9:145-152.
33. Benchimol S. p53-dependent pathways of apoptosis. Cell Death Differ 2001; 8:1049-10451.
34. Khaw AK, Hande MP, Kalthur G, Hande MP. Curcumin inhibits telomerase and induces telomere shortening and apoptosis in brain tumour cells. J Cell Bbiochem 2013; 114:1257-1270.
35. Noorafshan A, Ashkani-Esfahani S. A review of therapeutic effects of curcumin. Curr Pharm Des 2013; 19:2032-2046.
36. Reuter S, Eifes S, Dicato M, Aggarwal BB, Diederich M. Modulation of anti-apoptotic and survival pathways by curcumin as a strategy to induce apoptosis in cancer cells. Biochem Pharmacol 2008; 76:1340-1351.
37. Jee SH, Shen SC, Kuo ML, Tseng CR, Chiu HC. Curcumin induces a p53-dependent apoptosis in human basal cell carcinoma cells.J Invest Dermatol 1998; 111:656-661.
38. Gomez-Manzano C, Fueyo J, Kyritsis AP, Steck PA, Roth JA, McDonnell TJ, *et al*. Adenovirus-mediated transfer of the p53 gene produces rapid and generalized death of human glioma cells via apoptosis. Cancer Res 1996; 56:694-699.
39. Sun Y. E3 ubiquitin ligases as cancer targets and biomarkers. Neoplasia 2006; 8:645-654.
40. Goel A, Kunnumakkara AB, Aggarwal BB. Curcumin as "Curecumin": from kitchen to clinic. Biochem Pharmacol 2008; 75:787-809.
41. Zerbini LF, Libermann TA. Life and death in cancer GADD45 α and γ are critical regulators of NF-κB mediated escape from programmed cell death. Cell Cycle 2005; 4:18-20.
42. Bales KR, Du Y, Dodel RC, Yan GM, Hamilton-Byrd E, Paul SM. The NF-κB/Rel family of proteins mediates Aβ-induced neurotoxicity and glial activation. Brain Res Mol Brain Res 1998; 57:63-72.
43. Guo Q, Robinson N, Mattson MP. Secreted β-amyloid precursor protein counteracts the proapoptotic action of mutant presenilin-1 by activation of NF-κB and stabilization of calcium homeostasis. J Biol Chem 1998; 273:12341-12351.
44. Gerondakis S, Grossmann M, Nakamura Y, Pohl T, Grumont R. Genetic approaches in mice to understand Rel/NF-kappaB and IkappaB function: transgenics and knockouts. Oncogene 1999; 18:6888-6895.
45. Mattson MP, Camandola S. NF-κB in neuronal plasticity and neurodegenerative disorders. J Clin Invest 2001; 107:247-254.
46. Chen F, Castranova V, Shi X. New insights into the role of nuclear factor-κB in cell growth regulation. Am J Pathol 2001; 159:387-397.
47. Kastan MB, Zhan Q, El-Deiry WS, Carrier F, Jacks T, Walsh WV, *et al*. A mammalian cell cycle checkpoint pathway utilizing p53 and GADD45 is defective in ataxia-telangiectasia. Cell 1992; 71:587-597.
48. Salvador JM, Brown-Clay JD, Fornace Jr AJ. Gadd45 in stress signaling, cell cycle control, and apoptosis. Adv Exp Med Biol 2013; 793:1-19.
49. Zerbini LF, Wang Y, Correa RG, Cho JY, Libermann TA. Blockage of NF-kappaB induces serine 15 phosphorylation of mutant p53 by JNK kinase in prostate cancer cells. Cell Cycle 2005; 4:1247-1253.
50. Hildesheim J, Bulavin DV, Anver MR, Alvord WG, Hollander MC, Vardanian L, *et al*. Gadd45a protects against UV irradiation-induced skin tumors, and promotes apoptosis and stress signaling via MAPK and p53. Cancer Res 2002; 62:7305-7315.
51. Tong T, Ji J, Jin S, Li X, Fan W, Song Y, *et al*. Gadd45a expression induces Bim dissociation from the cytoskeleton and translocation to mitochondria. Mol Cell Biol 2005; 25:4488-4500.